

Full sky study of diffuse Galactic emission at decimeter wavelengths

<https://doi.org/10.1051/0004-6361:20031125>

University of São Paulo
Nicolli Soares P.

CONTENTS

- Introduction and objectives
- Data description
- Description of the destriping method
- Spectral index and normalization maps
- Discussion and conclusions

Introduction and objectives

- Diffuse galactic emission at the frequencies studied in this article has as its main component synchrotron radiation
- Observations suffer from many systematic effects which depend on the specific experimental setup and observing strategies. In addition to there being a need to unite observations from different instruments
- Apply a cleaning algorithm to three largest low frequency maps: the 408 MHz map by Haslam et al. (1982), the 1420 MHz map from Reich (1982) and Reich & Reich (1986), and the 2326 MHz map by Jonas et al. (1998).

Introduction and objectives

- Build reliable models of the spectral index (beta) and power-law normalization factor (alpha) of galactic emission.
- Any template of the Galactic emission is frequency dependent (Wilkinson Microwave Anisotropy Probe (WMAP) results).

$$T_v = \alpha v^{-\beta}$$

Power law of Galactic emission

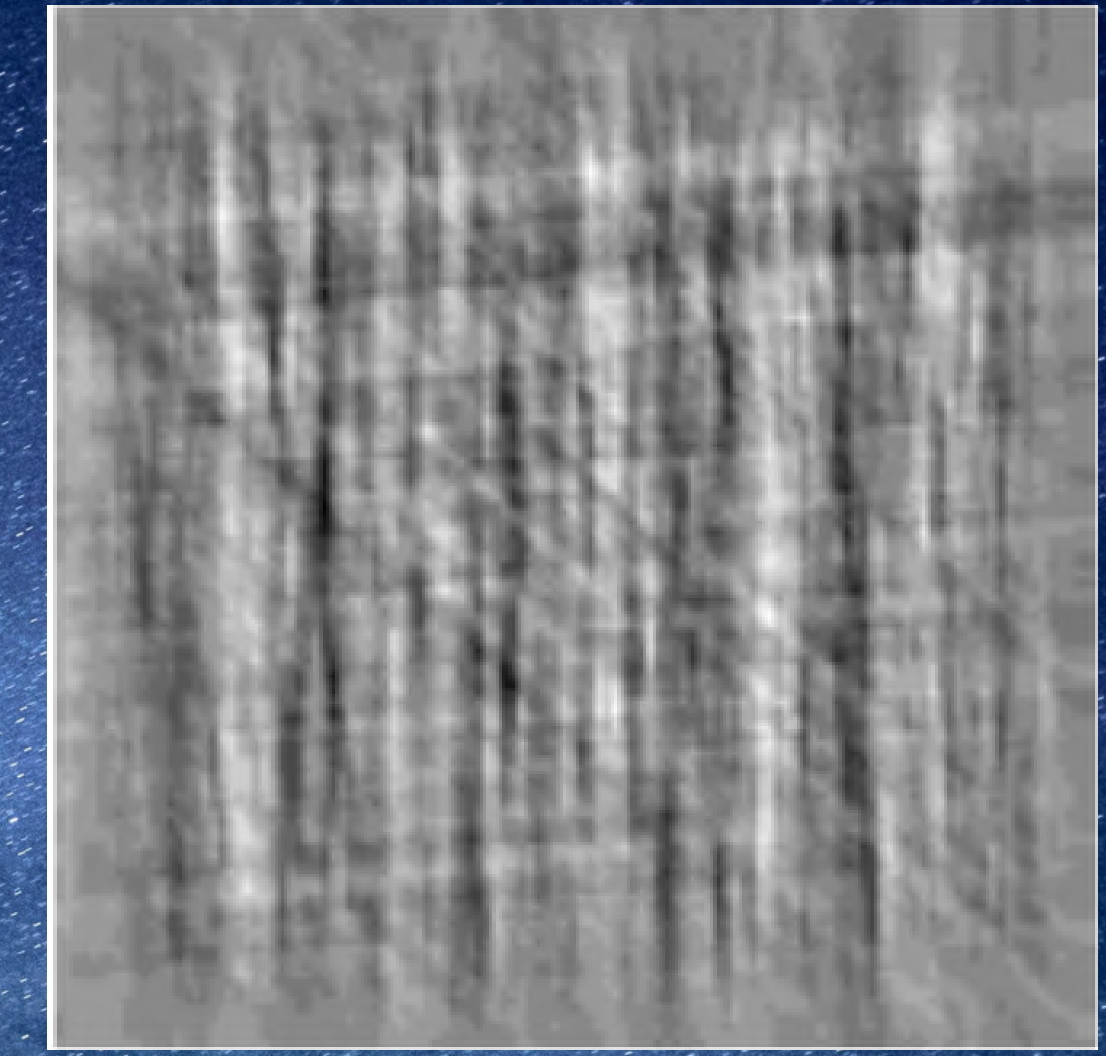
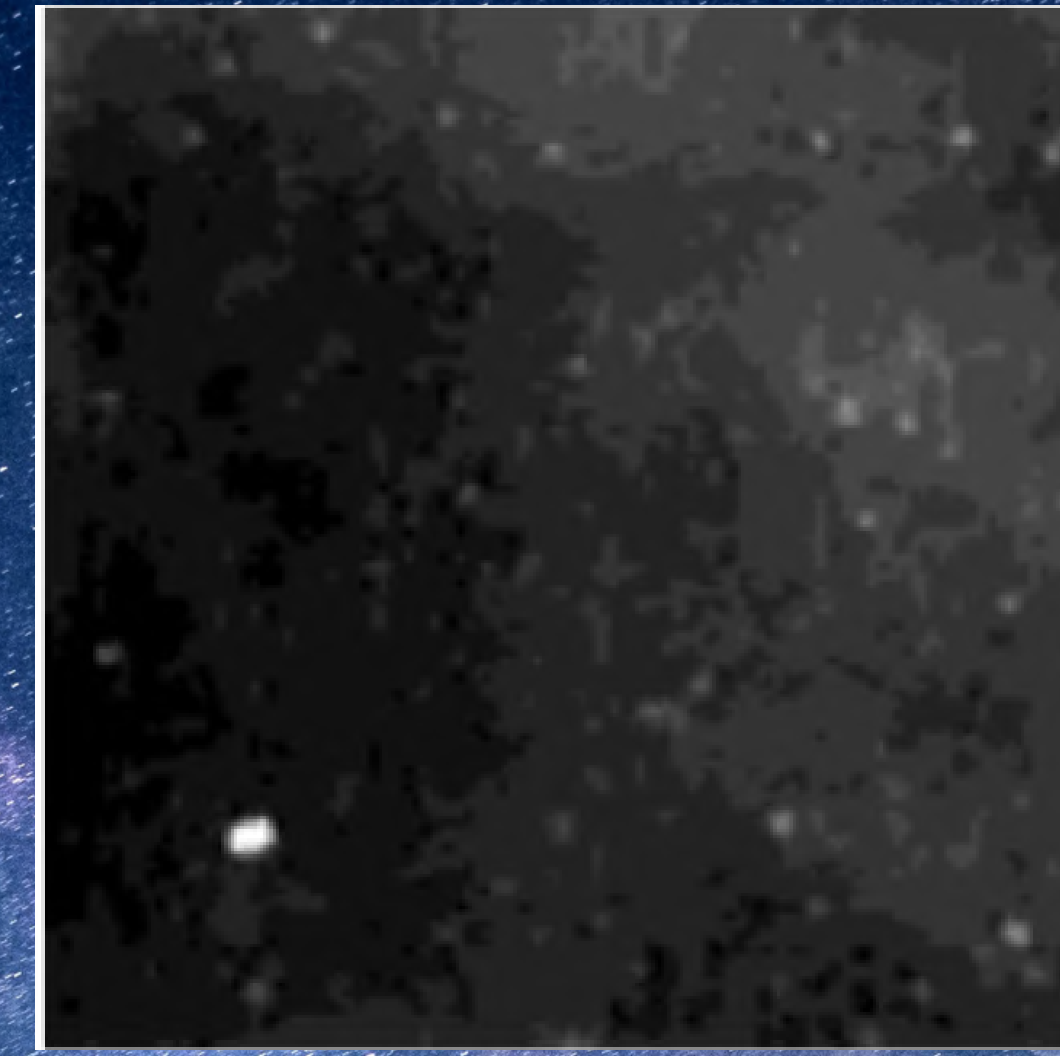
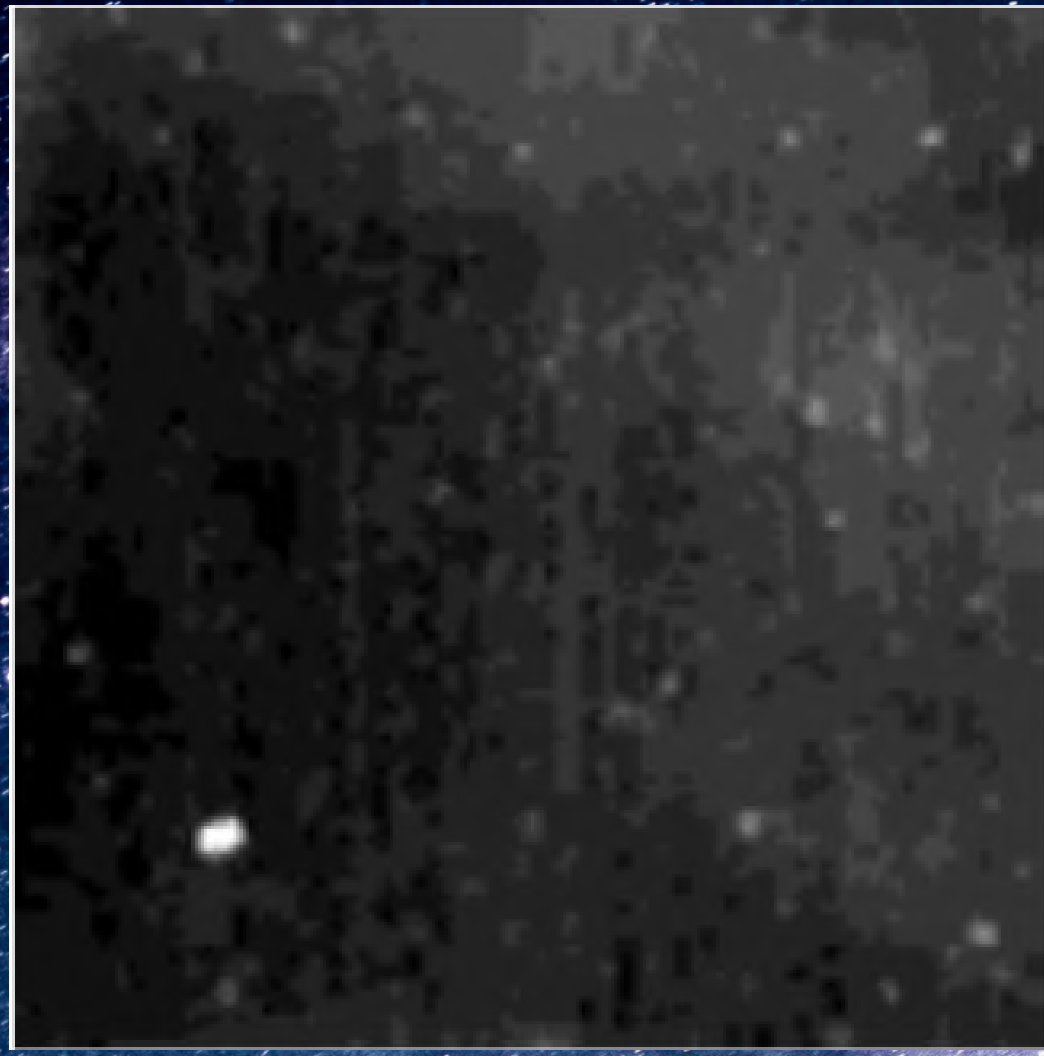
Data description

- Spectral index varies reflecting the variation in electron density and magnetic field, therefore a realistic model must take this into account, in addition to the changes that occur as a result of increasing frequency

Survey	calibration error (per cent)	Zero level error (K)	Baseline correction	Extragalactic background (K)
Frequency (MHz)				
408	10	3	–	5.92
1420	5	0.5	-0.13	2.83
2326	5	0.080	–	2.75

Parameters from
the original
experiments at 408,
142 and 2326 MHz

- From these three surveys we have 3 final maps, 408 MHz, 1420 MHz, 2326 MHz.
- 408 MHz: the map features nearly vertical stripes generated by the elevation sweep strategy and some diagonal lines.
- 1420 MHz: the inclined lines here reflect the azimuth scanning strategy, the authors also remove some diagonal and horizontal lines, and leave spurious structures less apparent.
- 2326 MHz: vertical lines are still visible even after the procedures applied by the authors



**At left patch of the 408 MHz map, in the middle the same destriped and
on the right the lines taken from the map**

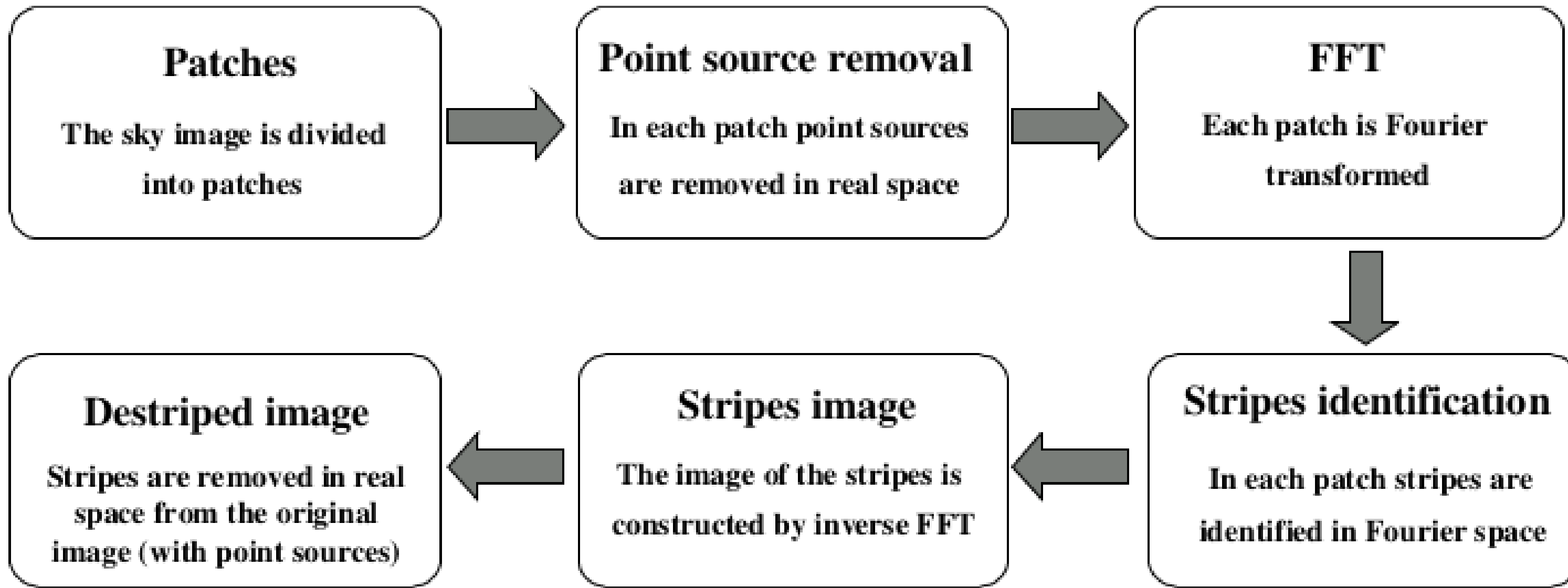
Description of the describing method

- To clean the mentioned artifacts it is necessary to identify the contaminated directions and remove excess signal
- The code acts on maps divided respectively into 44, 33, and 22 parts of 152×152 pixels.

$$\Delta\theta \times \Delta\phi = (0.35 \times 0.35) \text{ degree}$$

angular size of the pixels

- Maps are used in polar coordinates, using an equi-cylindrical projection (ECP) pixelization.



Overview of the process

- The regions where there are point sources to be removed are determined by a certain threshold
- The source signal is then replaced with the median signal from an annulus around the source (SFD); this allows stripping to be performed in the Fourier space

$$(k_r, k_\theta)$$

Parameterization in polar coordinates, the space is divided into 90 bins of 2-degree in k theta coordinate

$$P_{back}$$

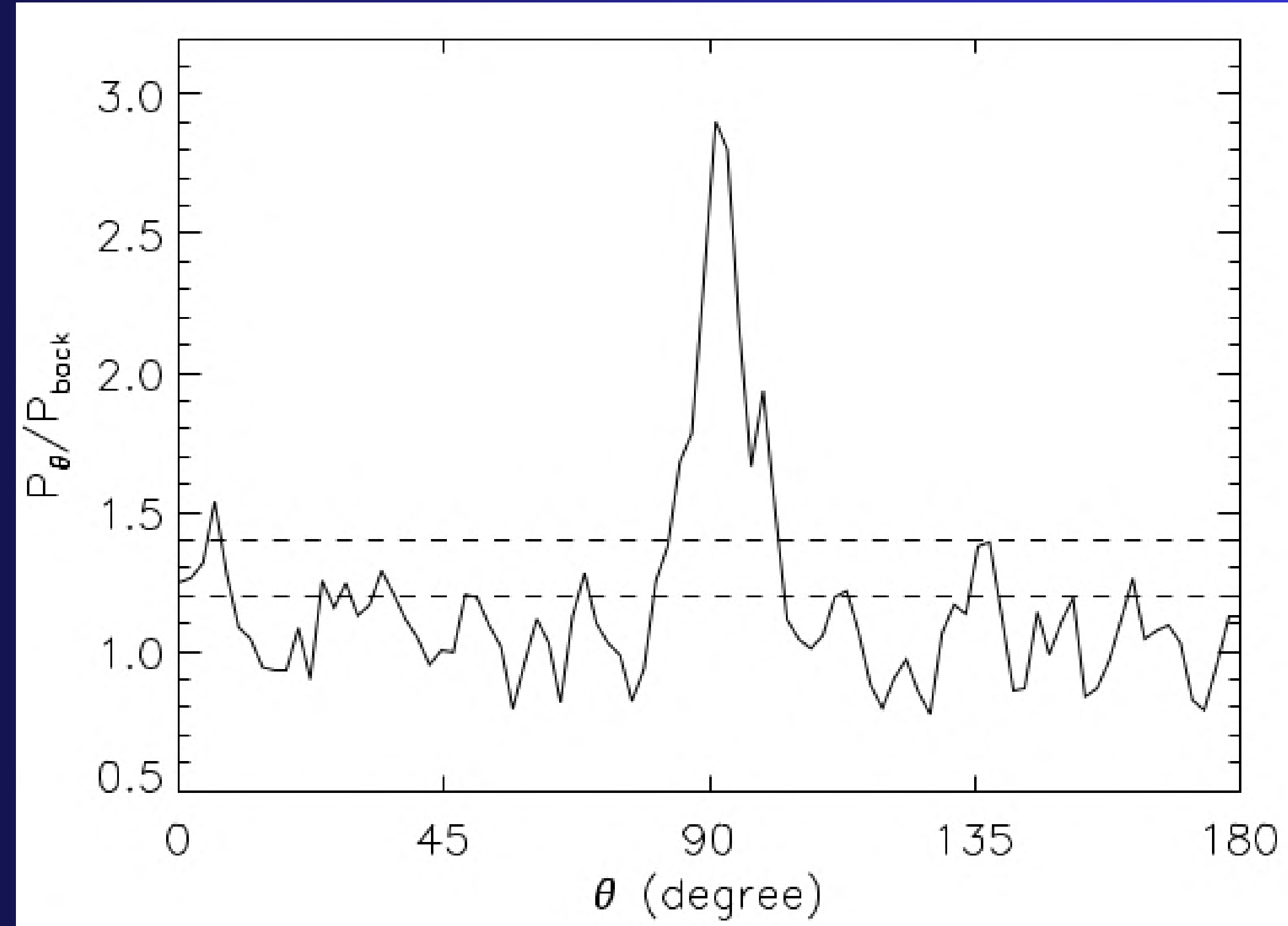
Background power is calculated using a Milky Way dust reddening map, the Schlegel–Finkbeiner–Davis (SFD) map.

$$\gamma_{\theta} = \frac{P_{\theta}}{P_{back}}$$

Parameterization in polar coordinates, the space is divided into 90 bins of 2-degree in k theta coordinate

$\bar{\gamma}$

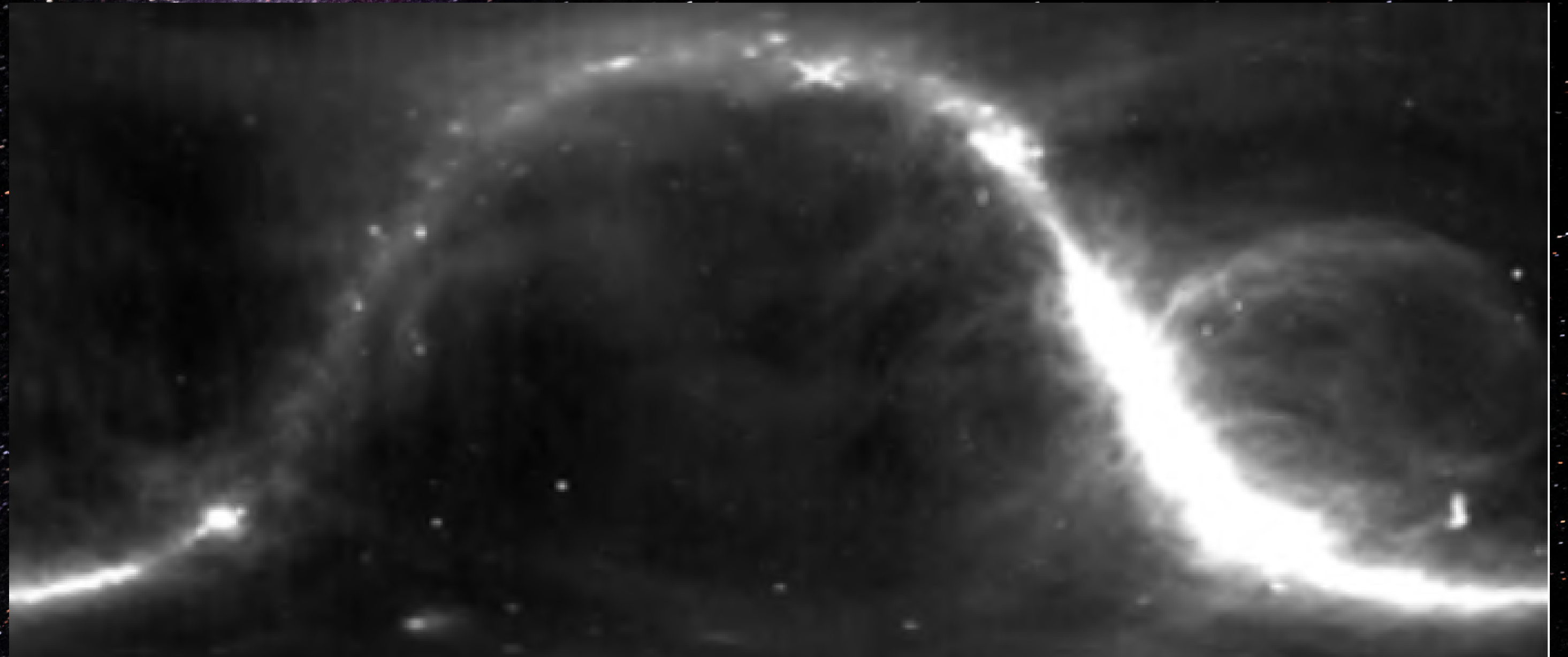
Dashed line



	$\delta T < 1\%$	$1\% < \delta T < 5\%$	$5\% < \delta T < 10\%$	$\delta T > 10\%$
408	36.4%	55%	7.0%	0.6%
1420	89.14%	10.7%	0.15%	0.01%
2326	18.3%	50.6%	22.5%	8.6%

Distribution of percentage temperature variation δT values in four different ranges and the corresponding pixel percentage. δT is evaluated as the difference after and before destriping.

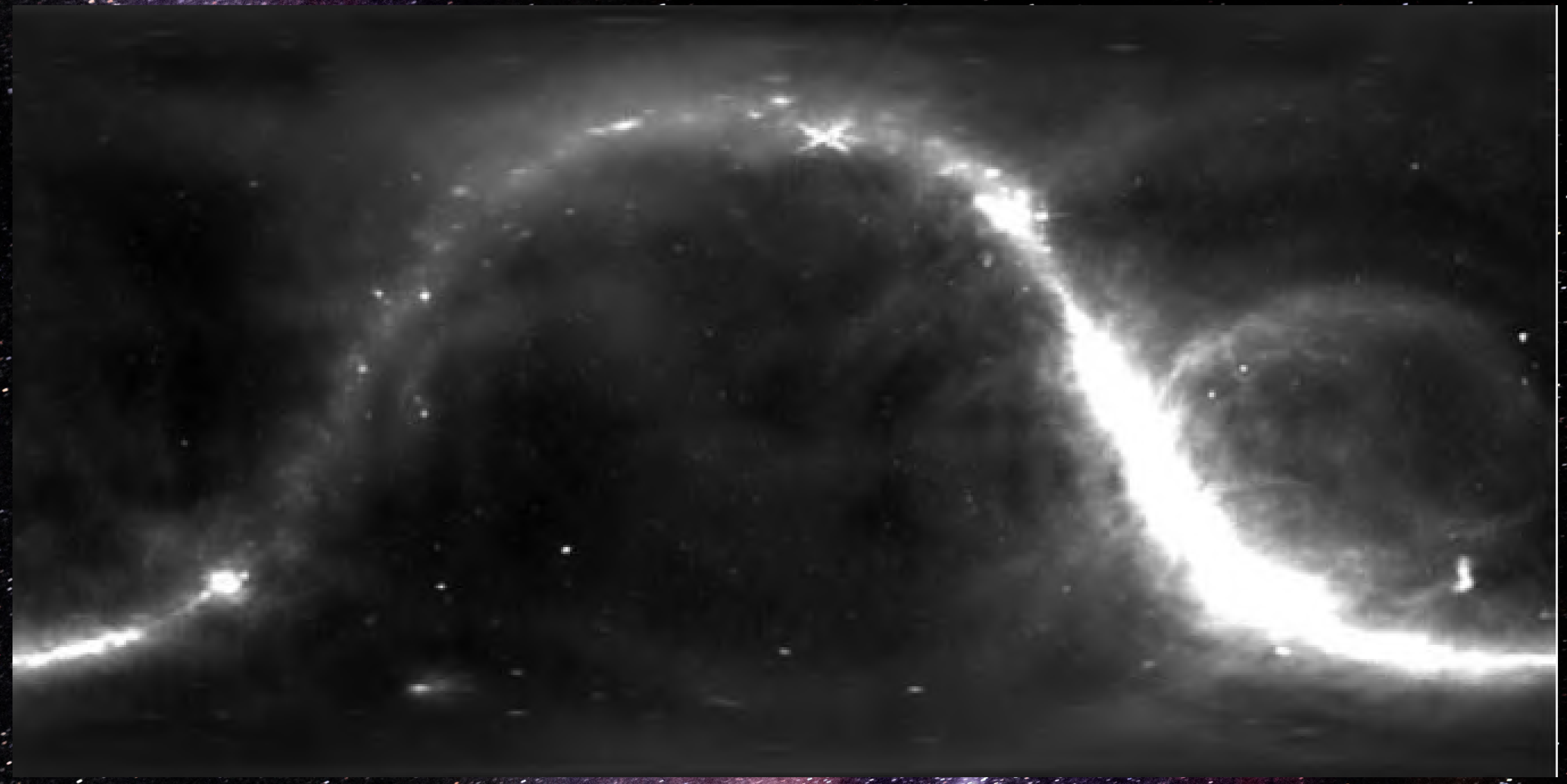
- The technique works well for isolated sources; in the case of extended structures, however, the replacement of the high source signal with the median background cause the smoothing of the structure borders.



Kelvin

10.872

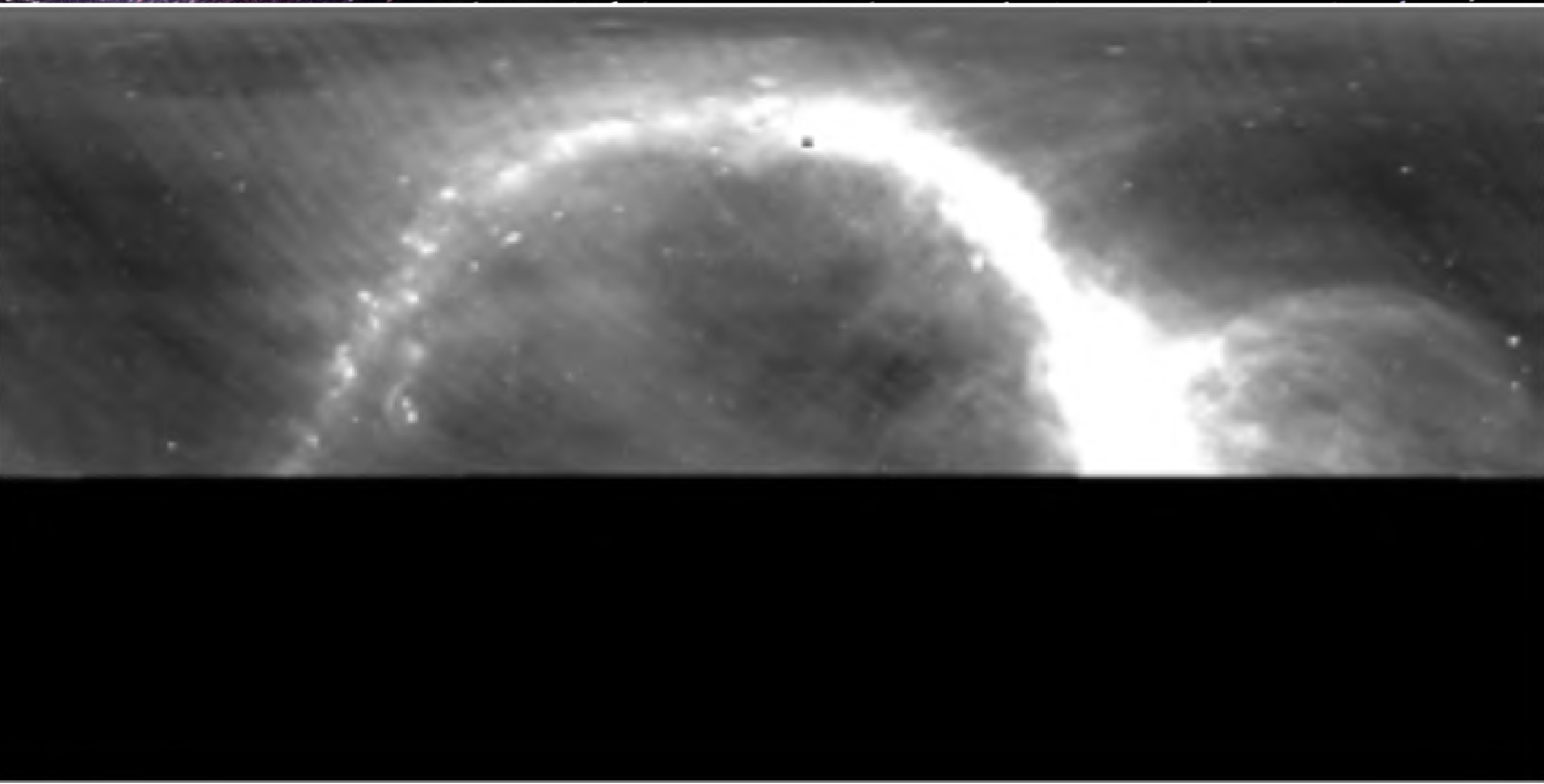
4246.993



Kelvin

10.872

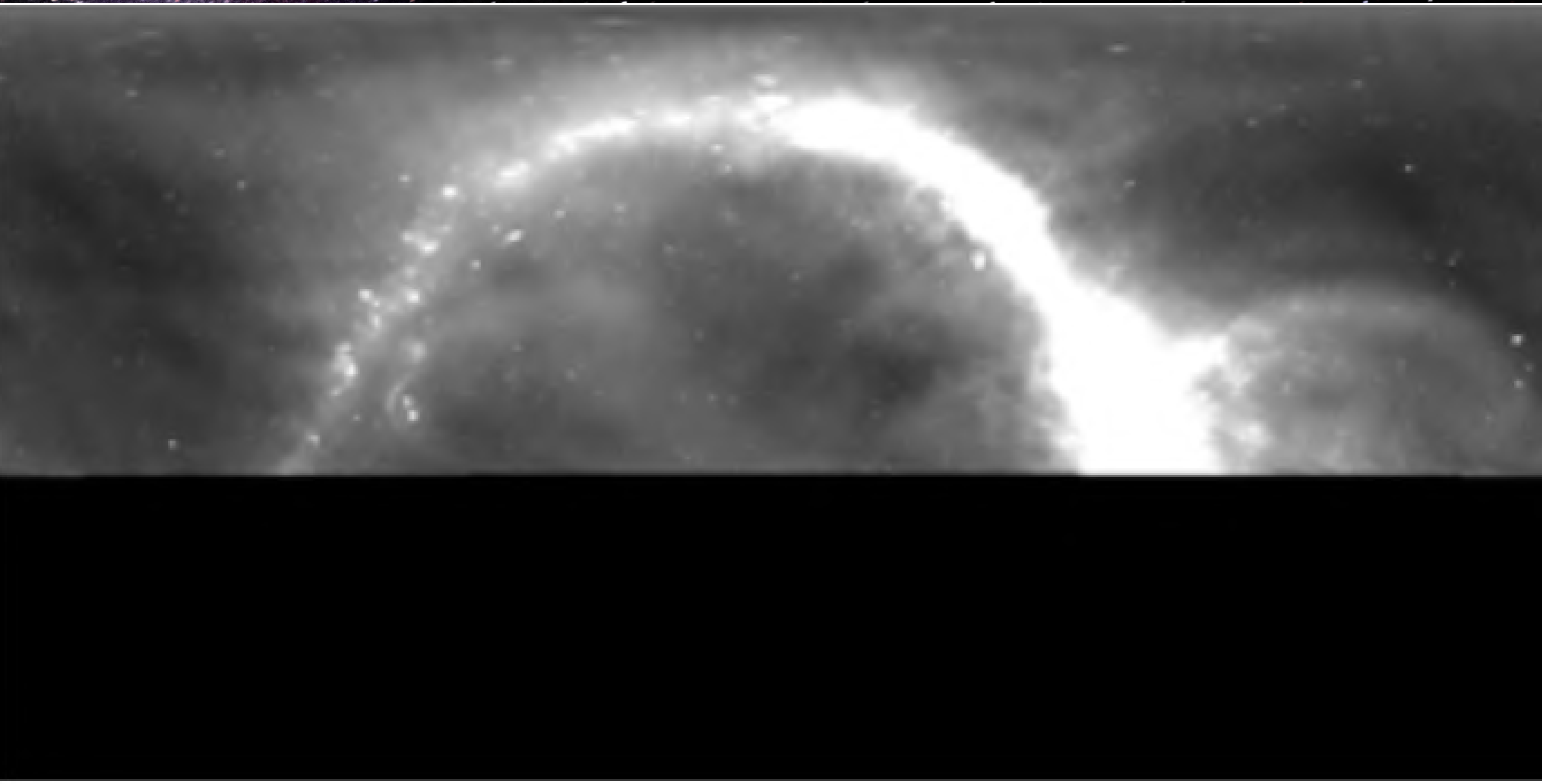
4246.993



Kelvin

3.163

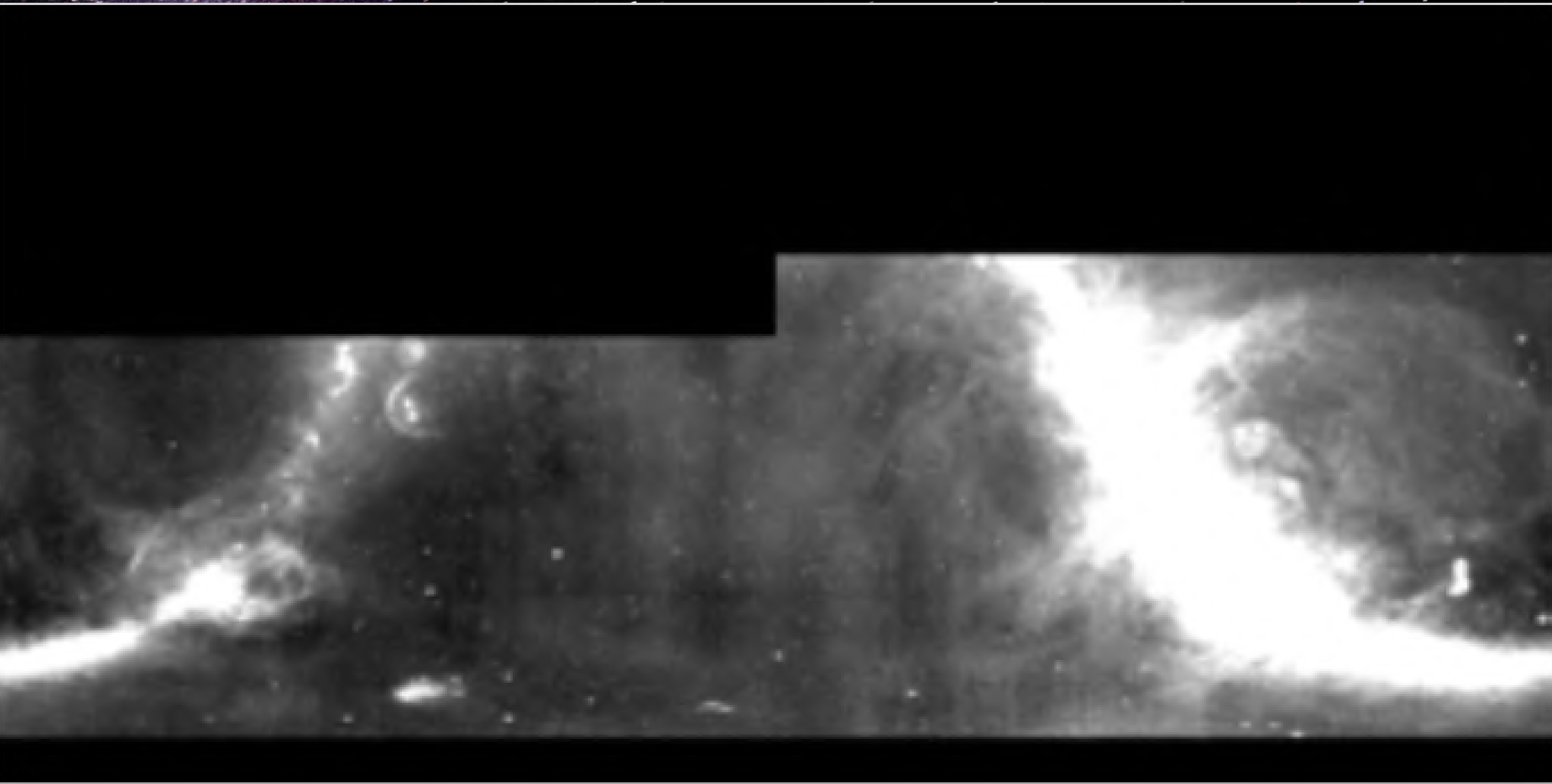
45.347



Kelvin

3.163

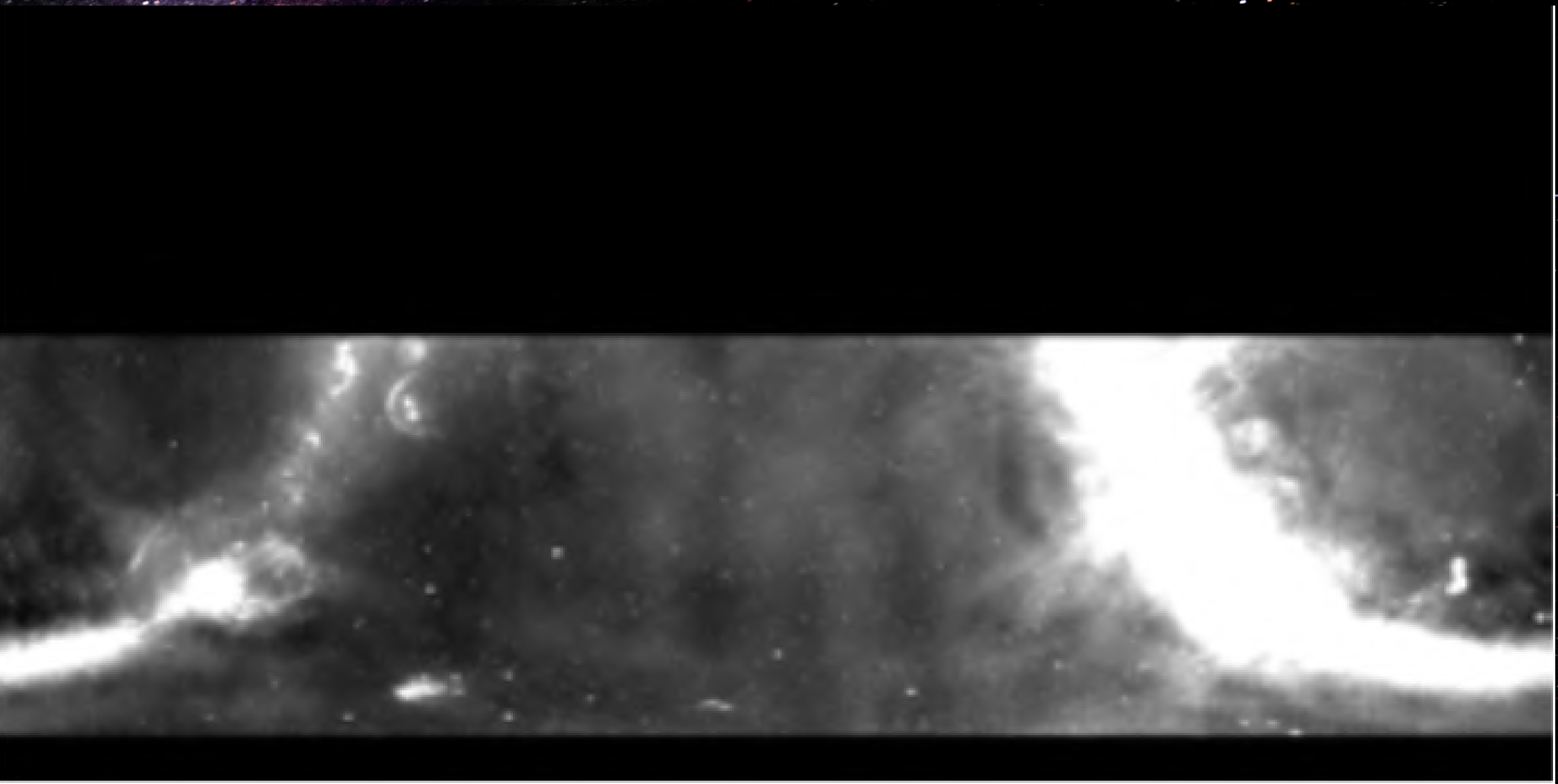
45.347



Kelvin

0.019

64.479



Kelvin

0.019

64.479

Spectral index and normalization factor maps

σ_{sens} δ_{0I} g_{cal}

$$C_a = L \sqrt{\sin \theta_i}$$

$$\theta_i = \pi - Li$$

$$\sigma_{pol,2326} = 20\%$$

- Quoted sensitivity
- Errors on the zero level
- Calibration
- A correction factor, C_a , to account for the different area of the pixels

- Error evaluation of the 2326 MHz temperature

$$dT_{408} = \left[(\sigma_{\text{sens},408} \theta_{408}^b / c_a)^2 + \delta_{01,408}^2 + (T_{408} g_{\text{cal},408})^2 \right]^{1/2}$$

- Power law of Galactic emission



$$dT_{1420} = \left[(\sigma_{\text{sens},1420} \theta_{1420}^b (\theta_{1420}^b / \theta_{408}^b) / c_a)^2 + \delta_{01,1420}^2 + (T_{1420} g_{\text{cal},1420})^2 \right]^{1/2}$$

$$\log T_\nu = \alpha - \beta \log \nu,$$

$$dT_{2326} = \left[(\sigma_{\text{sens},2326} \theta_{2326}^b (\theta_{2326}^b / \theta_{408}^b) / c_a)^2 + \delta_{01,2326}^2 + (T_{2326} g_{\text{cal},2326})^2 + (T_{2326} \sigma_{\text{pol},2326})^2 \right]^{1/2}$$

Spectral index, normalization factor and their uncertainties

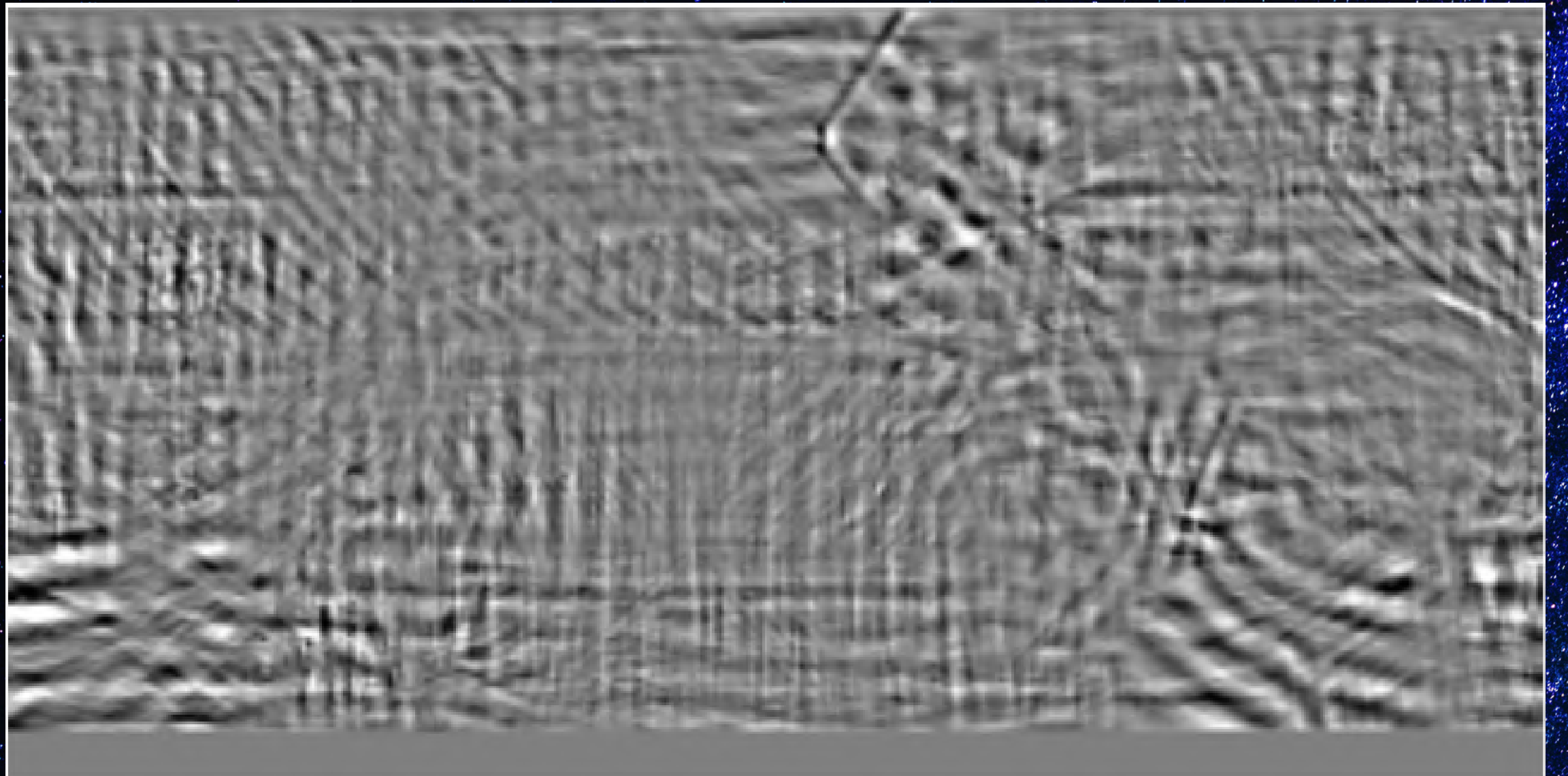
$$\beta_{\nu_1/\nu_2} = -\frac{\log(T_{\nu_1}/T_{\nu_2})}{\log(\nu_1/\nu_2)},$$

$$\alpha = \frac{\log \nu_1 \log T_{\nu_2} - \log \nu_2 \log T_{\nu_1}}{\log \nu_1 - \log \nu_2},$$

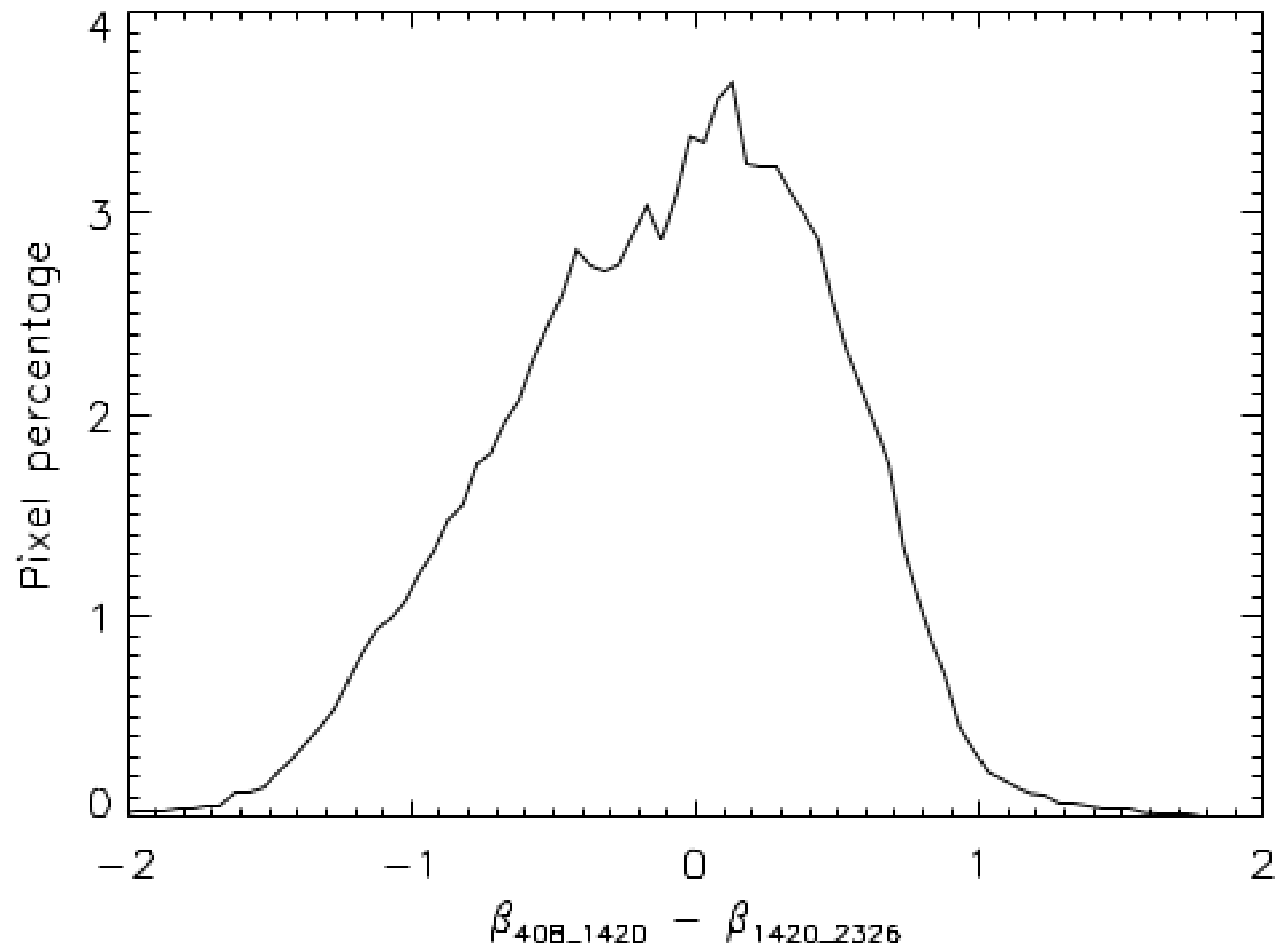
$$\sigma_\beta = |\log \nu_1 - \log \nu_2|^{-1} \sqrt{\left(\frac{dT_1}{T_1 \log 10}\right)^2 + \left(\frac{dT_2}{T_2 \log 10}\right)^2}$$

$$\begin{aligned} \sigma_\alpha &= |\log \nu_1 - \log \nu_2|^{-1} \\ &\times \sqrt{\nu_2^2 \left(\frac{dT_1}{T_1 \log 10}\right)^2 + \nu_1^2 \left(\frac{dT_2}{T_2 \log 10}\right)^2}. \end{aligned}$$

**Map of the differences $D\beta$
between the spectral
index evaluated with the
destriped and the original
maps**



Comparison of β (408,1420) with β (1420,2326)



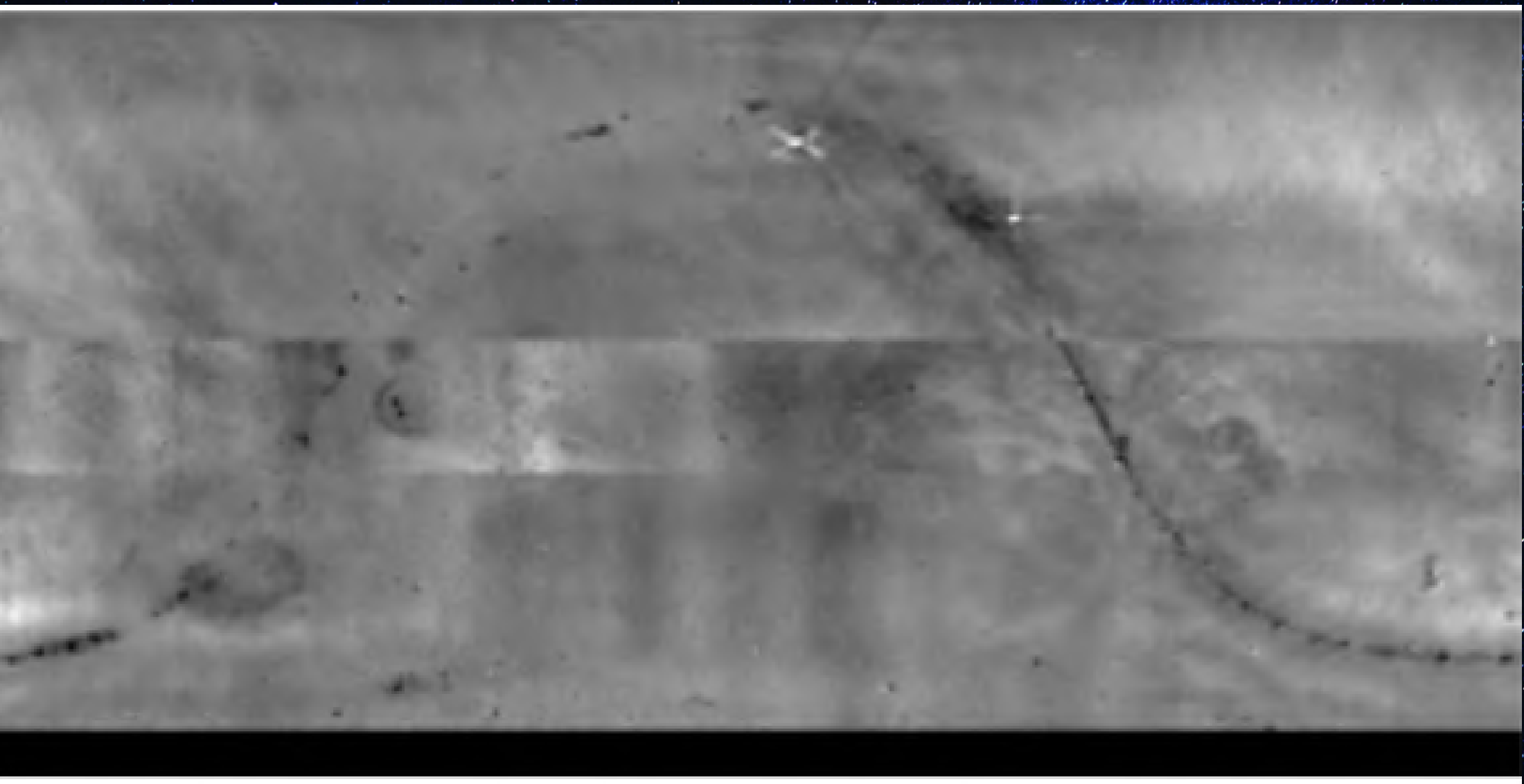
- The estimated error is greater than the frequency variation of the spectral index β between 1420 and 2326 MHz.
- Use all three searches to get a single map of spectral indices and frequency normalization factors range 408–2326 MHz.

- There are discontinuities at the frequency edges 1420 and 2326 MHz
- The discontinuities in the α and β maps could be accounted for within the quoted measurements systematic errors of the three surveys, gain and zero-level errors.
- With a combination of six parameters (three pairs of parameters, calibration factor g_{cal} and zero level correction δ_{0I} , each for each frequency map) to rescale the maps to account for their zero level and calibration errors with the aim to minimize the difference across the discontinuities.
- The six parameters influence the β and α values through the optimized temperatures of the maps

$$T_{v_{optimized}} = T_{v_{g_{cal}}} + \delta_{0I}$$

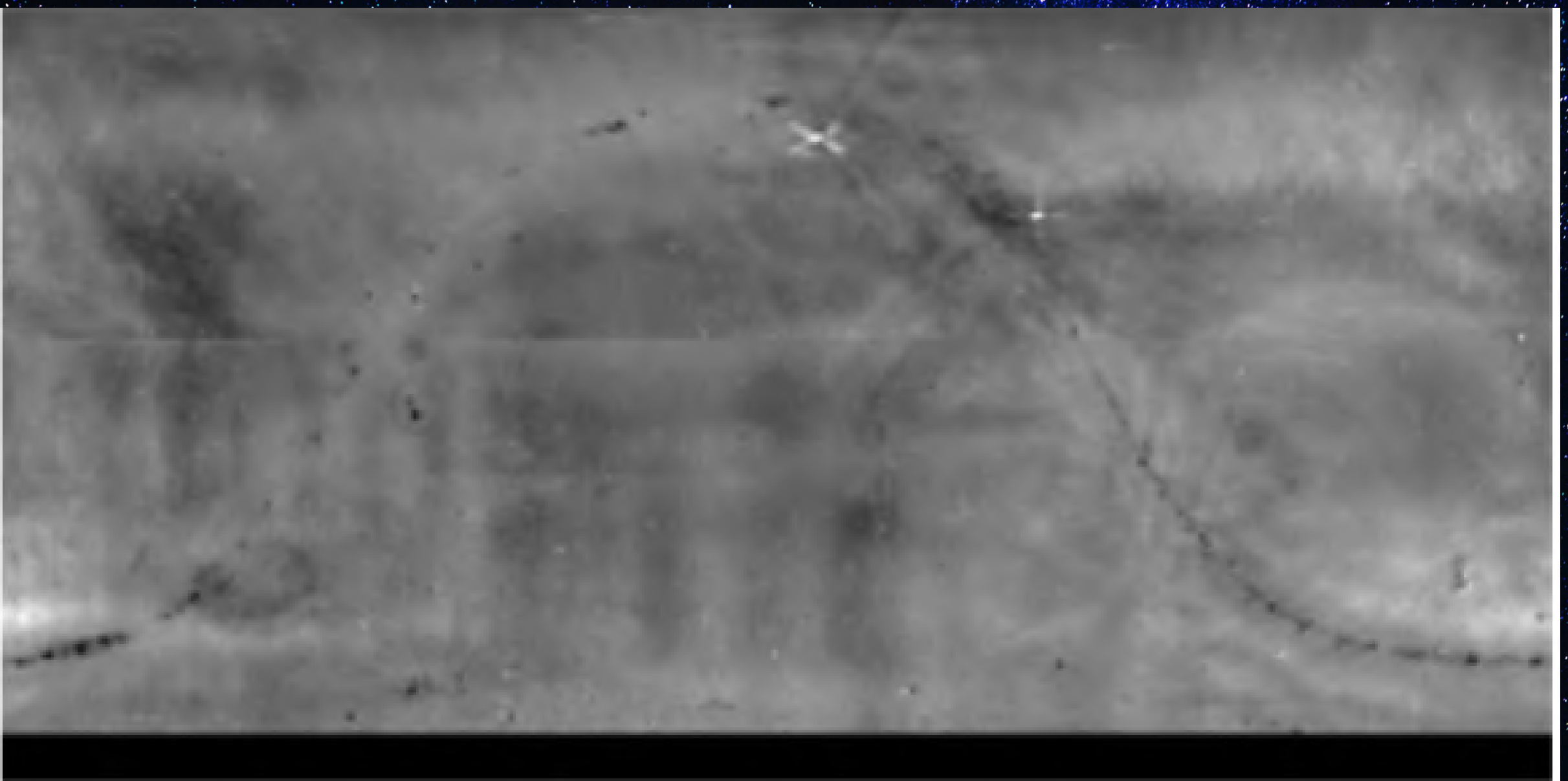
$$\chi^2 = \sum_{i=1}^N \frac{(\beta_{2d}(i) - \beta_{3d}(i))^2}{\sigma_{\beta_{2d}}^2(i) + \sigma_{\beta_{3d}}^2(i)} + \frac{(\beta_{2u}(i) - \beta_{3u}(i))^2}{\sigma_{\beta_{2u}}^2(i) + \sigma_{\beta_{3u}}^2(i)} \\ + \frac{(\alpha_{2d}(i) - \alpha_{3d}(i))^2}{\sigma_{\alpha_{2d}}^2(i) + \sigma_{\alpha_{3d}}^2(i)} + \frac{(\alpha_{2u}(i) - \alpha_{3u}(i))^2}{\sigma_{\alpha_{2u}}^2(i) + \sigma_{\alpha_{3u}}^2(i)},$$

Expression that minimizes the power law parameters, where “u” and “d” refer to the up and down discontinuities respectively, the low indices 2 and 3 refer to β and α evaluated by exploring two or three frequency maps, and the sum is carried out over i th azimuthal position of all the Ω pixels of the top and bottom border lines of the overlapping region.



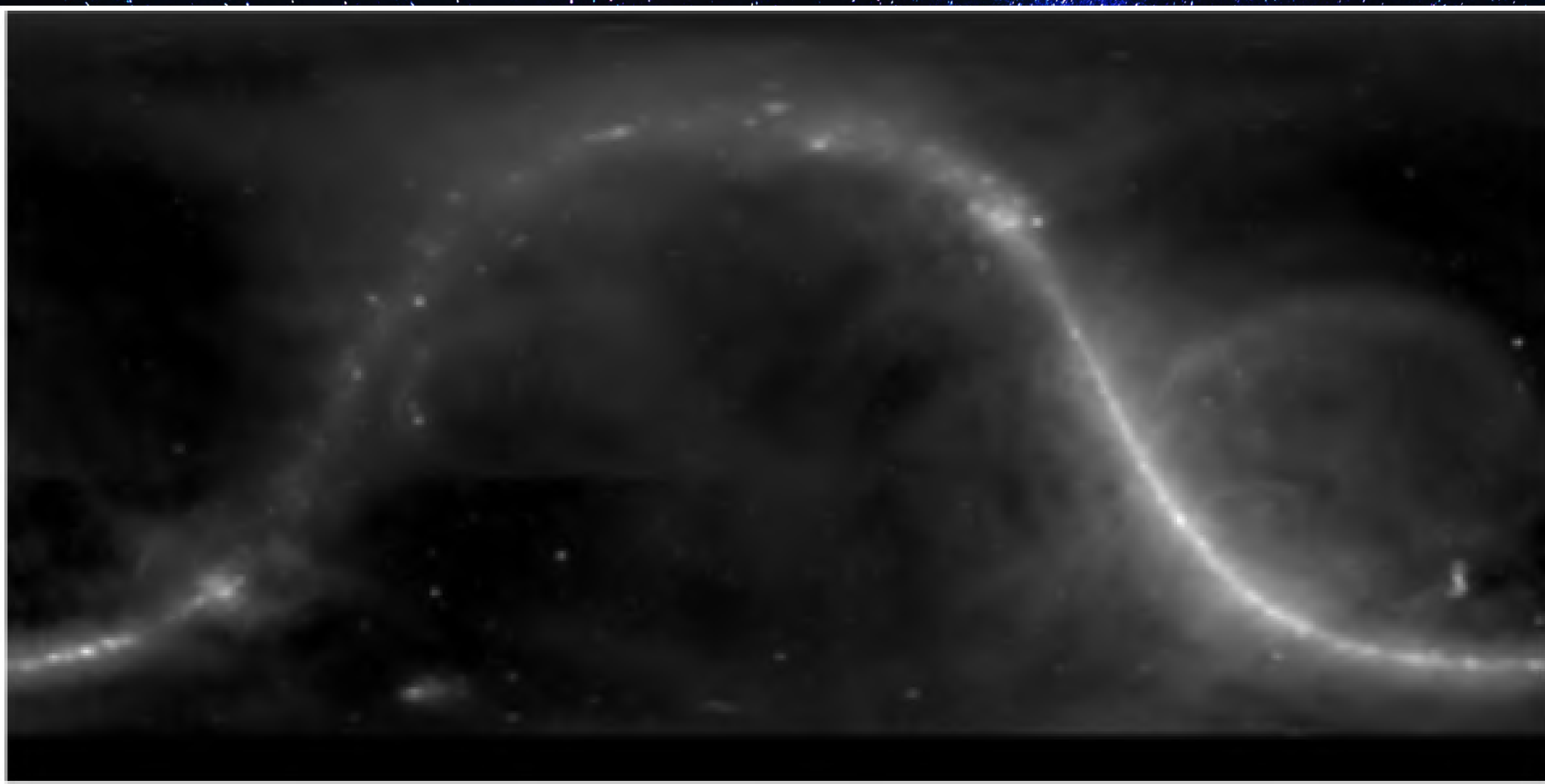
2.000

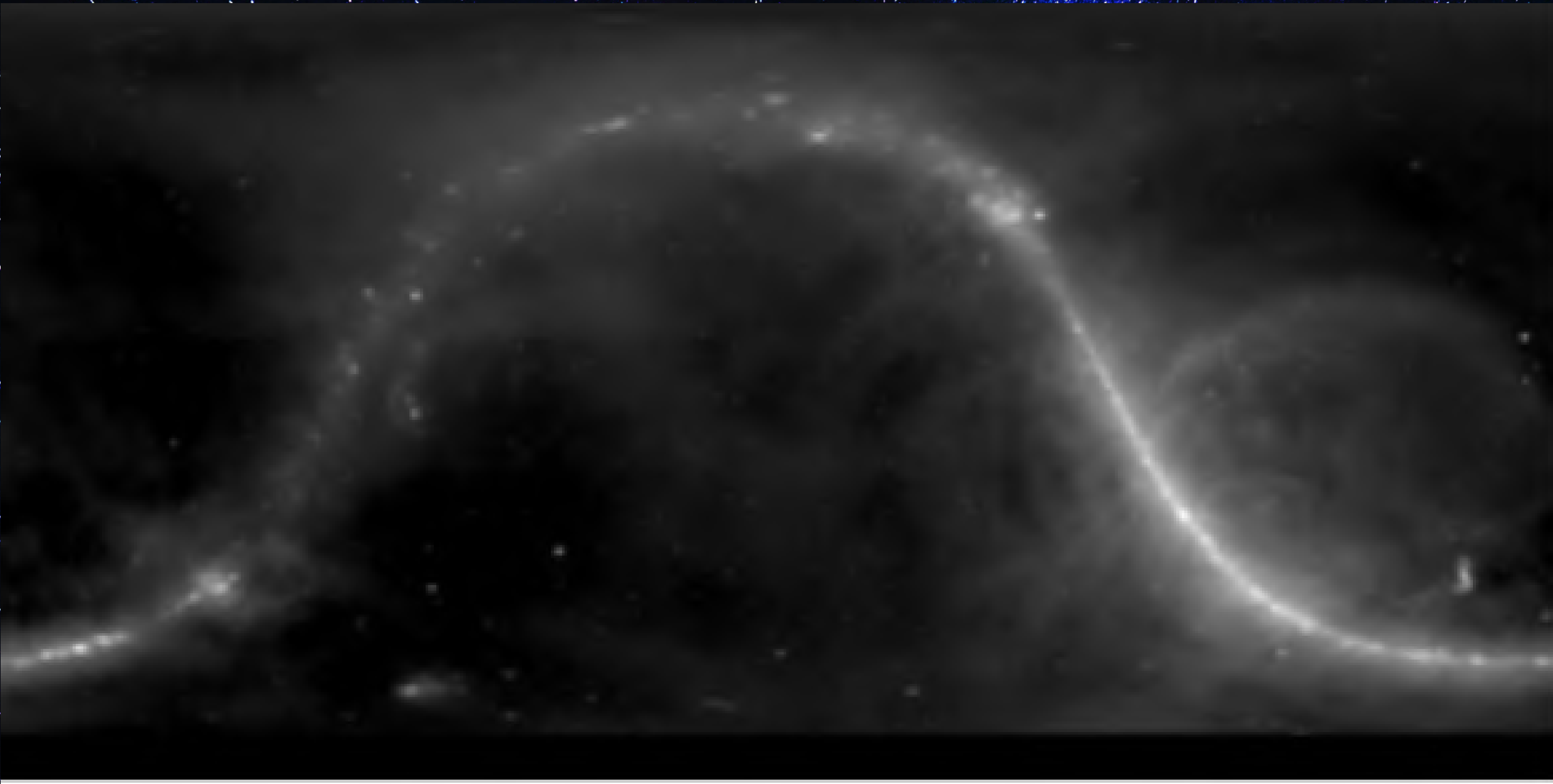
3.500



2.000

3.500

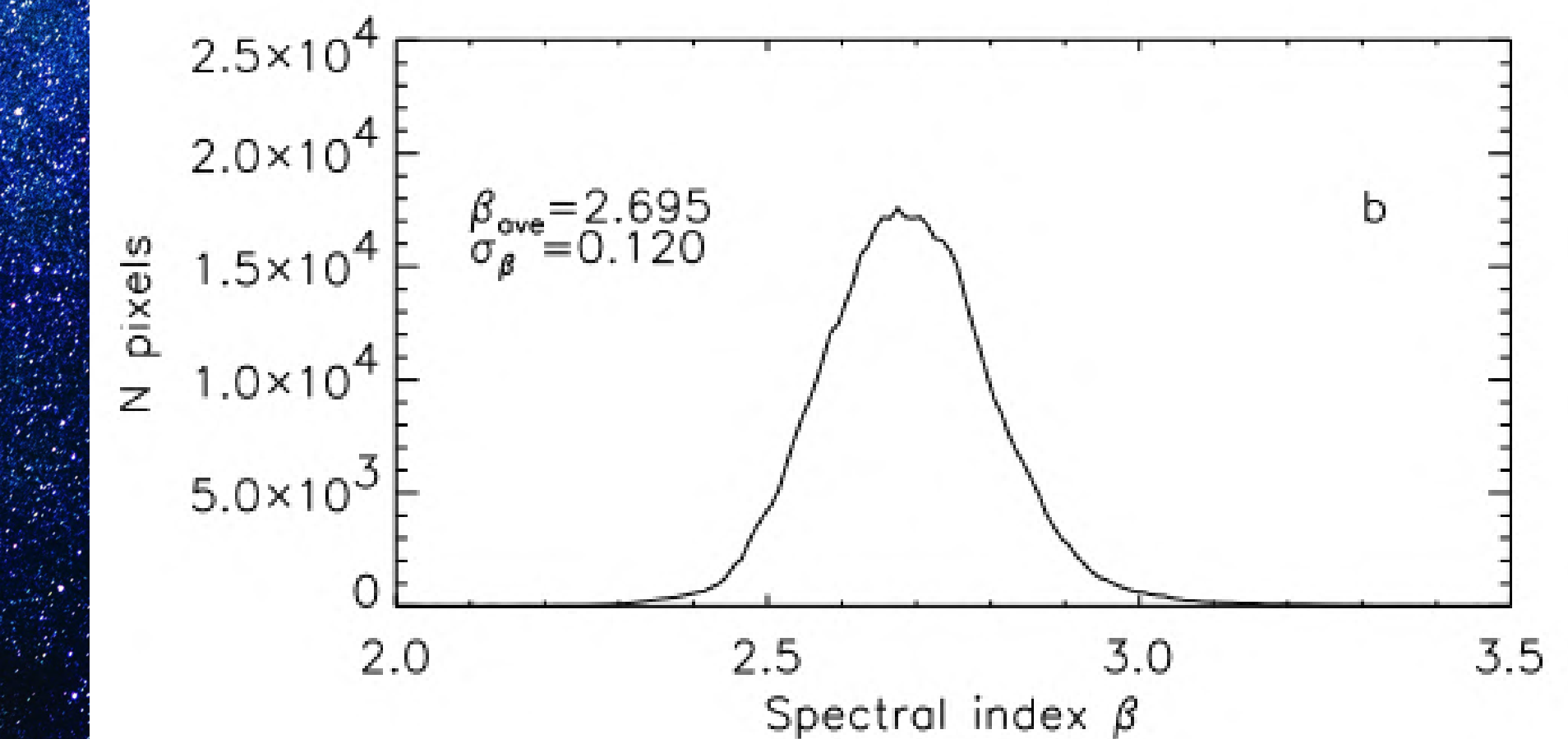
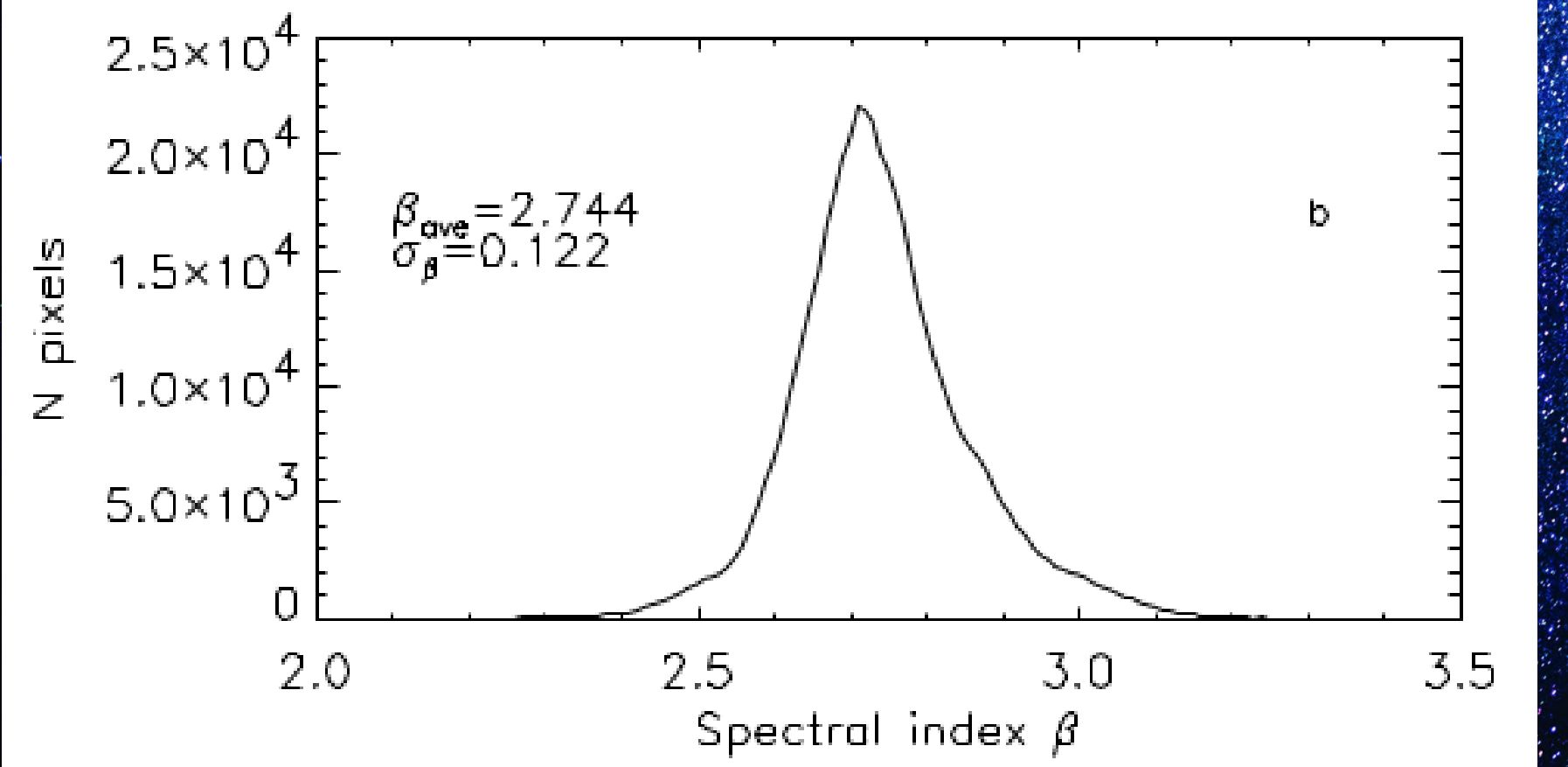
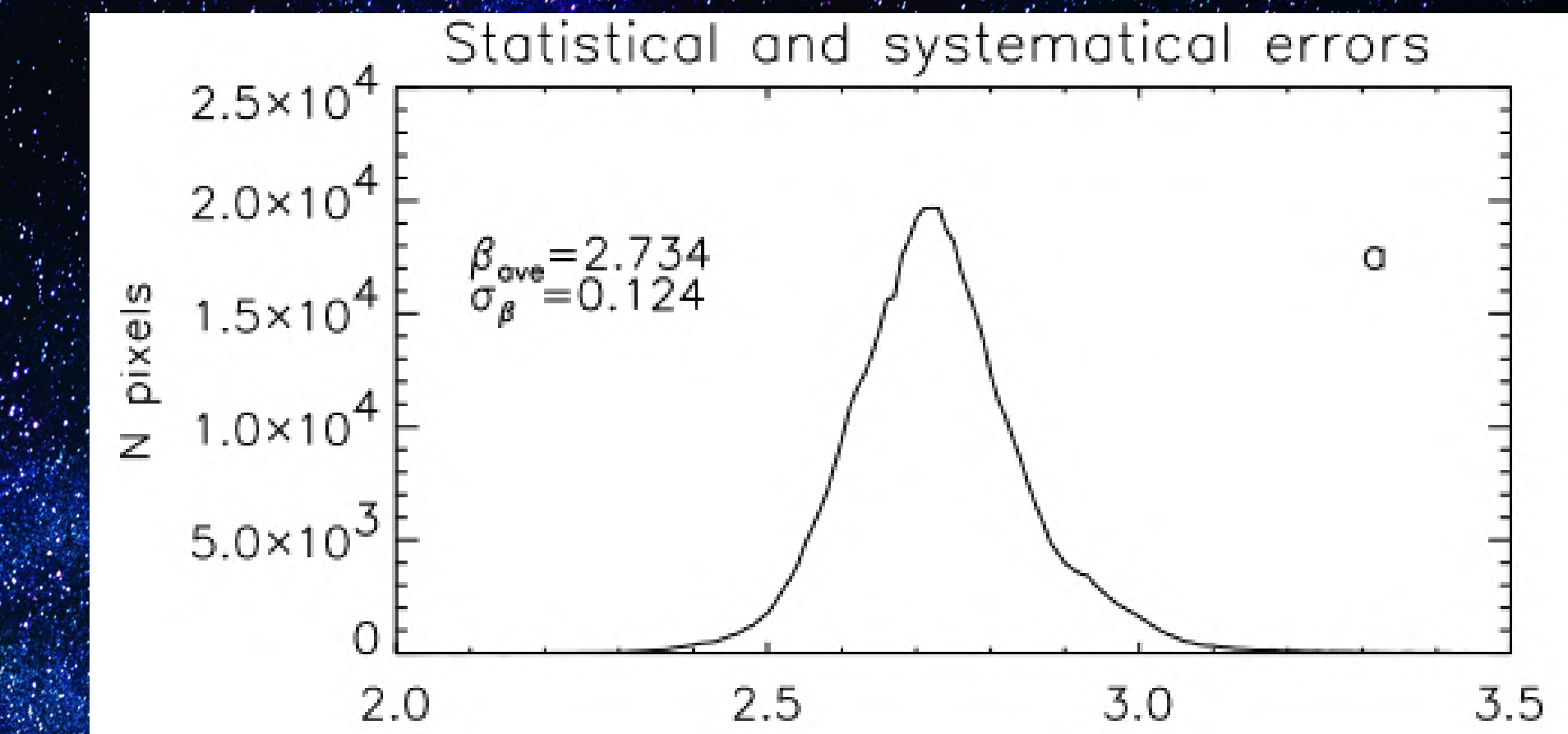
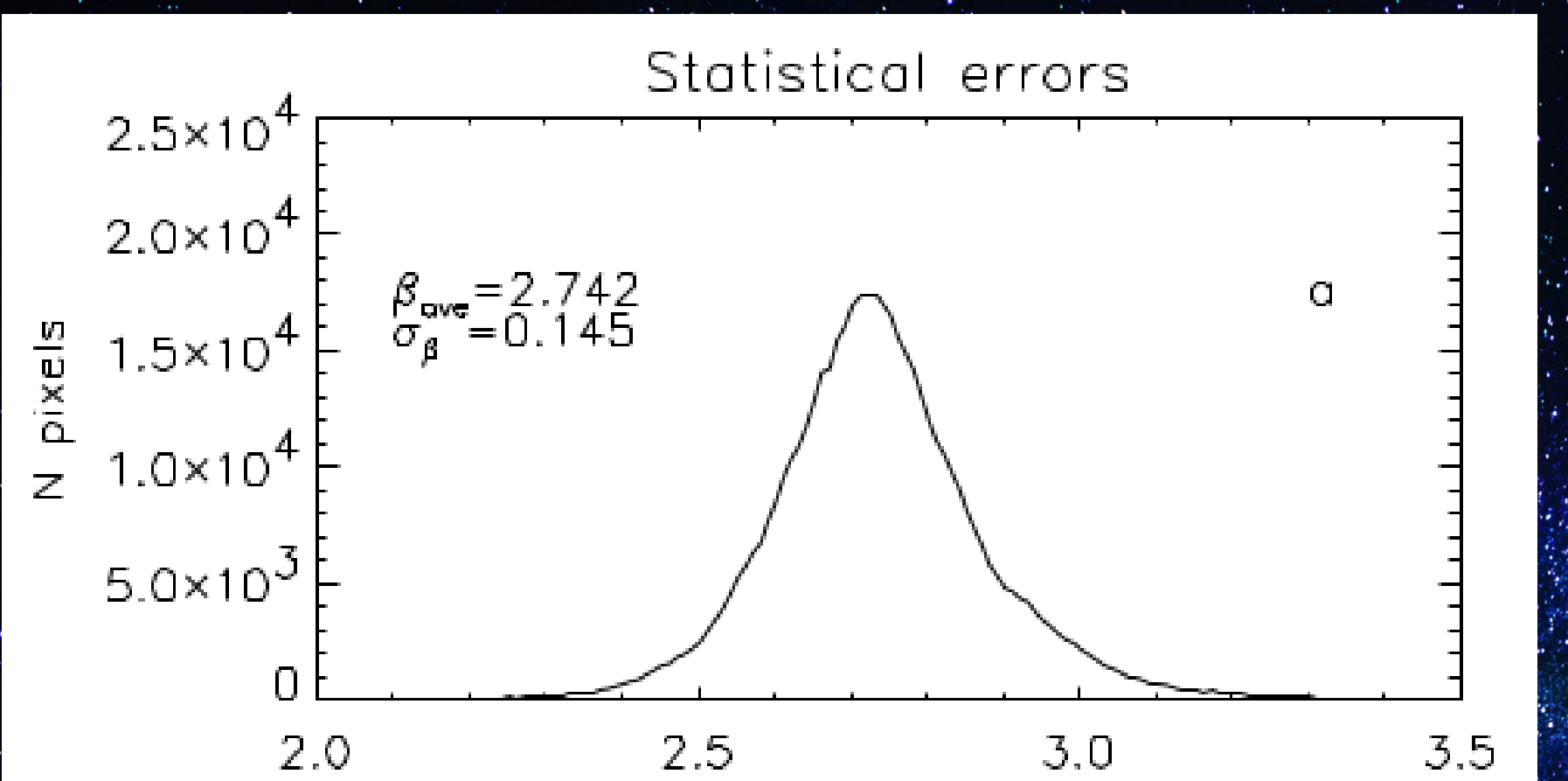




- Calibration factors and zero level corrections for the three maps as recovered after the minimization for statistical errors only and with systematic errors includes

	statistical errors only	statistical + systematic errors
$g_{\text{cal},408}$	0.877	0.973
$g_{\text{cal},1420}$	1.100	1.066
$g_{\text{cal},2326}$	0.827	0.793
$\delta_{01,408}$	3.432 K	0.676 K
$\delta_{01,1420}$	-0.0410 K	-0.0267 K
$\delta_{01,2326}$	0.0366 K	0.0357 K
$\chi^2/\text{d.o.f.}$	14.381	0.204

		statistical errors only	statistical + systematic errors
before minimization	$\bar{\beta} \pm \sigma_\beta$	2.742 ± 0.145	2.734 ± 0.124
	%pixels with $\beta < 2$	0.031	0.015
	%pixels with $\beta > 3.5$	0.066	0.05
after minimization	$\bar{\beta} \pm \sigma_\beta$	2.744 ± 0.122	2.695 ± 0.120
	%pixels with $\beta < 2$	0.022	0.009
	%pixels with $\beta > 3.5$	0.012	0.012



- The contribution of point sources to the spectral index was estimated by subtracting point sources from maps without stripes, the result was that this procedure can smooth the edges of the maps
- The diffuse Galactic maps resulting from this work are representative for synchrotron spectral index distribution and synchrotron normalization factor. Point sources contribution is limited to a small number of pixels that could be isolated and removed to extrapolate the maps at high frequency and obtain synchrotron emission templates.

Discussion and Conclusions

Thank you